

## Optimization of Polysulfone/Polyethylene Glycol (PSf/PEG) Casted Solution Composition as a Membrane Electrolyte in a Dye-Sensitized Solar Cell (DSSC)

Sinta Anjas Cahyani, Nita Kusumawati\*

Department of Chemistry, Faculty of Mathematics and Natural Sciences, Universitas Negeri Surabaya, Surabaya, Indonesia

\*E-mail: [nitakusumawati@unesa.ac.id](mailto:nitakusumawati@unesa.ac.id)

Received: March 5, 2024. Accepted: April 29, 2024. Published: May 25, 2024

**Abstract:** Stability is the main challenge in developing electrical energy made from sunlight, namely Dye-Sensitized Solar Cell (DSSC). The DSSC system comprises a photoanode, electrolyte, comparison electrode, and dye sensitizer with a photoelectrochemical working principle. Dye sensitizer and electrolyte are the main components that determine the stability of DSSC, with problems such as solvent evaporation leakage in liquid electrolytes and dye desorption. In overcoming these problems, the polymer electrolyte of Polysulfone/Polyethylene Glycol (PSf/PEG) is a solution to the problem by increasing the mobility of  $I^-/I_3^-$  ions in the electrolyte. Polymer composition and porogen (pore formers) affect the ionic conductivity, which impacts the electron flow of the DSSC system. Therefore, this study optimized the composition of PSf/PEG polymer electrolyte, namely 18/0, 17/1, 16/2, 15/3, 14/4, and 13/5. This research was carried out using quantitative methods with data processed in a quantitative descriptive manner to determine the performance of DSSC based on PSf/PEG membrane electrolyte. The wavelength absorption of the dye was characterized using a Spectrophotometer UV-Vis instrument, and the specific wavelength was obtained at 573 nm, which indicates anthocyanin absorption. Electrochemical characterization of the dye using voltammetry yielded a resulting energy bandgap value of 0.5132 eV with the touch plot method. Testing the performance and stability of DSSC, voltage, and current measurements were carried out using a multimeter, and fill factor and efficiency calculations were carried out. The performance of DSSC with liquid electrolytes was 1.66%, while that of DSSC with membrane electrolytes of the best composition (16/2) was 1.38% at 0 hours. In addition, the performance test was carried out at 72 hours of exposure time, resulting in an efficiency of 0.77%, while the DSSC with the best composition of membrane electrolyte (16/2) was 1.11%. This shows a decrease in the efficiency of DSSC with liquid electrolytes by 53.43%, while the membrane electrolyte efficiency of DSSC is 19.33-20.17%.

**Keywords:** DSSC; Membrane Electrolyte; PSf/PEG; Stability.

### Introduction

The energy demand worldwide continues to increase as the world's population grows, industry develops, and technology advances. Energy needs must be met to maintain economic, political, and environmental stability. So far, the world's energy needs are highly dependent on fossil fuels such as oil, coal, and natural gas, with a usage percentage of 37%, 27%, and 36%, respectively. However, using fossil fuels can trigger anthropogenic global warming and damage the environment. In addition, the increase in demand for fossil fuels, which is not proportional to their limited availability, can trigger the problem of a lack of energy supply. As a solution, alternative renewable energy with abundant availability is needed, such as solar energy, which can be harvested using solar cells [1].

Solar cells are an abundant and easy-to-use renewable resource for energy needs [2-3]. DSSC is one of the technologies that can convert light energy into electrical energy using the photovoltaic effect [4]. DSSC attracts the attention of researchers because of its advantages in simple and economical fabrication, as well as the availability of materials that are easy to find compared to Silicon Solar Cell (SSC) [5]. DSSC has four essential parts in its basic structure: the working electrode or photoanode, dye

sensitizer, electrolyte, and comparison electrode or photocathode [6].

Dye sensitizers are one of the main components that affect the efficiency of DSSCs [7-9]. To produce high efficiency, the dye sensitizer must have a broad and robust absorption profile to obtain optimum photon harvesting from solar irradiation [10-11]. Several studies report using synthetic dyes such as ruthenium as dye sensitizers. Although it produces high efficiency, ruthenium is challenging to synthesize, expensive, and toxic. As an alternative, natural dyes can be used as photosensitizers. Several studies report using synthetic dyes such as ruthenium as dye sensitizers [12]. Although it produces high efficiency, ruthenium is challenging to synthesize, expensive, and toxic. As an alternative, natural dyes can be used as photosensitizers.

Photosensitizers can come from chlorophyll, carotene, anthocyanin, tannin, and flavonoid pigments obtained from plant parts, such as leaves, flowers, fruits, roots, stems, seeds, and skin [13]. One of the flowers that can be used as a photosensitizer is the butterfly pea (*Clitoria ternatea*), which has a characteristic single petal in blue, purple, white, and pink [14]. Butterfly pea is a plant that contains anthocyanin pigments and has bluish-purple color characteristics after the extraction process [15]. Research by Ludin et al. (2018) reported that the fabrication

### How to Cite:

Cahyani, S. A., & Kusumawati, N. (2024). Optimization of Polysulfone/Polyethylene Glycol (PSf/PEG) Casted Solution Composition as a Membrane Electrolyte in a Dye-Sensitized Solar Cell (DSSC). *Jurnal Pijar Mipa*, 19(3), 499–506. <https://doi.org/10.29303/jpm.v19i3.6610>

of DSSC with anthocyanin pigments from butterfly pea extract can produce an efficiency of 0.13% [16]. Thus, natural photosensitizers from butterfly pea extract have the potential to produce DSSCs with high efficiency [17-18].

In addition to the dye sensitizer, DSSC performance is also determined by the electrolyte, which is responsible for transporting charge from the photoanode to the comparison electrode. High-efficiency DSSCs are generally produced by liquid electrolytes with  $I^-/I_3^-$  redox pairs dissolved in volatile organic solvents. However, the liquid electrolyte's high solvent evaporation and leakage limit its further utilization. As a solution, polymer-based electrolytes were developed with the advantages of high ionic conductivity and flexible production scale [19]. It was reported in the research of Kusumawati et al. (2023) that the use of solid polymers (membranes) as a liquid electrolyte matrix can prevent electrolyte leakage and produce an efficiency of 1.23% [18]. Therefore, in this research, a Polysulfone (PSf) polymer-based electrolyte will be developed to be used as a porous separator or liquid electrolyte matrix due to its outstanding electrochemical stability, mechanical properties, and thermal characteristics [20]. The ability of PSf polymer in the form of a thin layer or membrane to trap liquid electrolyte ( $I^-/I_3^-$ ) will reduce solvent evaporation and liquid electrolyte leakage.

To get the best function as a liquid electrolyte matrix, it is essential to obtain suitable pore characteristics, which are small enough to hold the liquid electrolyte but also large enough to ensure no obstacles for the movement of electrons in the system. Besides size, the number of pores also determines the effectiveness of the PSf membrane as a liquid electrolyte matrix. One way that can be done to increase the porosity of the PSf membrane is by adding a porogen, such as Polyethylene glycol (PEG), which is mixed with the PSf polymer [21]. PEG can be used as a pore-forming PSf membrane because of its water-soluble ability to dissolve in polar solvents and good compatibility to suppress macrovoid formation [22].

This study evaluates the performance of DSSC with PSf/PEG polymer electrolyte using a multimeter to determine open-circuit voltage ( $V_{oc}$ ), short-circuit current density ( $J_{sc}$ ), fill factor (FF), and efficiency ( $\eta$ ). The performance of polymer electrolyte-based DSSCs is then compared with that of liquid electrolyte-based DSSCs to determine their effectiveness.

Therefore, the urgency of this research lies in global energy needs, which continue to increase along with world population growth, industrial development and technological advances. High dependence on fossil fuels such as petroleum, coal and natural gas to meet energy needs threatens economic and political stability and has severe environmental impacts, including anthropogenic global warming. As a solution, this research proposes the development of dye-sensitized solar cell (DSSC) technology by utilizing a natural sensitizer from butterfly pea (*Clitoria ternatea*) extract as well as the development of a polymer-based electrolyte, which is expected to overcome the limitations of conventional solar cell technology and encourage the widespread adoption of renewable energy. Wide.

## Research Methods

### Materials

The sensitizer materials include butterfly pea (*Clitoria ternatea*) and distilled water as a solvent. Iodine (99.8%, Sigma Aldrich), potassium iodide (99%, Merck), ethylene carbonate (99% anhydrous, Sigma Aldrich), and propylene carbonate (99.7% anhydrous, Sigma Aldrich) were used in making the electrolyte solution. Titanium(IV) oxide (particle size 21 nm, 99.5%, Sigma Aldrich), nitric acid (99.9%, Sigma Aldrich), polyethylene glycol-1000 (Merck), and Tween-80 (PT. Brataco Chemica) were used in the preparation of  $TiO_2$  paste. In addition, Polysulfone (PSf) (Mw 35,000; Sigma Aldrich) and DMAc (88%, Merck) were also used as membrane materials and Fluorine Doped Tin Oxide (FTO) glass (10  $\Omega$ , thickness 2.2 mm, size 2.5 x 2.5  $cm^2$ ) as conductive glass in the DSSC circuit.

### Methods

#### Preparation of Photosensitizer

Photosensitizers are obtained from the extraction of dried butterfly peas using the maceration method. At first, the dried butterfly peas were cut into small pieces using scissors. Then, extraction uses the maceration method with the solute to distilled water solvent ratio, namely 1:6 for 60 minutes. After 60 minutes, it is filtered with filter paper to obtain the bay flower dye filtrate, ready to be applied as a photosensitizer in a DSSC circuit [18].

#### Making $TiO_2$ Paste

Titanium dioxide ( $TiO_2$ ) paste as a layer on FTO glass is used as a working electrode in the DSSC circuit.  $TiO_2$  paste was made by weighing 0.2 grams of titanium dioxide ( $TiO_2$ ) powder and 0.08 grams of PEG-1000 using an analytical balance and placing it in a beaker. 0.05 mL of tween 80 and 0.4 mL of 0.1 M nitric acid ( $HNO_3$ ) were added as solvents. Next, stirred using a magnetic hotplate stirrer at 100 rpm for 30 minutes [18].

#### Working Electrode Preparation (Photoanode)

Before being coated with  $TiO_2$  paste, the FTO glass first determines the conductive parts using a multimeter, then divides them with tape; the sides are 2.5x2.5  $cm^2$  to form a square. Next, the  $TiO_2$  paste is coated on the FTO glass using the doctor blade method, which is then deposited on the conductive glass and smoothed using a spatula. After drying, the tape was removed from the FTO glass and heated using a hotplate at 450  $^\circ C$  for 1 hour. Next, the FTO glass coated with  $TiO_2$  is left to cool and used for immersion using dye from butterfly pea flower extract [18].

#### Preparation of Electrolyte Solution

To make the electrolyte solution, start by weighing 0.0092 grams of iodine ( $I_2$ ), 0.06 grams of potassium iodide (KI), 0.4 grams of propylene carbonate (PC), and 0.4 grams of ethylene carbonate (EC) solution, which is then added into a beaker and stirred using a magnetic hotplate stirrer at a speed of 100 rpm for 30 minutes [18].

## Preparation of PSf/PEG Polymer

Making the PSf/PEG polymer solution begins by weighing 5 grams of DMAc solution, as well as PSf and PEG powders with varying compositions (M0, M1, M2, M3, M4, and M5), then putting the ingredients into a beaker and stirring using a magnetic hotplate stirrer with speed of 270 rpm at a temperature of 60 °C for 90 minutes.

The polymer solution was cast using the casting knife method on glass measuring 14x14 cm<sup>2</sup> with an immersion temperature of 30 °C for 30 minutes. The solid PSf/PEG membrane was washed using 500 mL of distilled water for 1 minute with two repetitions. Then, the PSf/PEG membrane was dried at room temperature for 24 hours.

## Making a Counter Electrode (Cathode)

The reference electrode is made by coating carbon on the conductive side of the FTO glass. Look for the side of the FTO glass first, then heat that side over a candle flame to get a layer of carbon. The heating lasts long until the glass layer is black and its thickness can be seen evenly.

## DSSC Fabrication

DSSC consists of FTO anode and FTO cathode glass and electrolytes arranged in a sandwich system. This research uses variations in PSf/PEG membrane composition as a trap for DSSC performance. For polymer membrane-based electrolytes, PSf/PEG membranes with a thickness of 0.2 mm and 2x1.5 cm<sup>2</sup> were soaked in 1 mL of electrolyte solution for 60 minutes. The anode FTO glass is coated with TiO<sub>2</sub> and washed in 10 mL of photosensitizer butterfly pea for 24 hours. Meanwhile, cathode FTO glass is FTO glass coated with carbon. A DSSC sandwich is made in the following sequence: FTO glass anode-electrolyte-FTO glass cathode [18].

## DSSC Characterization

In this research, the characterization was carried out using UV-Vis spectrophotometry to measure the wavelength absorption of photosensitizers. Next, cyclic voltammetry is used for energy bandgap analysis of the photosensitizer. The solid PSf/PEG polymer layer morphology was observed using an optical microscope with SEM instruments. XRD crystallinity analysis was carried out to determine the level of regularity of the atomic/molecular structure that makes up the PSf/PEG polymer layer. On the DSSC circuit, measurements were carried out using a multimeter (resistance 200 kΩ and voltage 200 mV) to obtain  $V_{oc}$ ,  $J_{sc}$ , fill factor, and efficiency ( $\eta$ ) values.

## Results and Discussion

### Spectrophotometer UV-Vis Analysis

Before being used as a natural dye, the extract was characterized using a Spectrophotometer UV-Vis instrument to determine the specific wavelength. Testing is carried out in the wavelength range of 400-800 nm because the requirements for dye sensitizers in DSSC must have a wavelength absorption area in the 400-800 nm range [23]. Butterfly pea extract has a characteristic purplish blue color and contains anthocyanin pigments [24]. Anthocyanins absorb visible light in the wavelength range from 480 to

580 nm [25-26]. Anthocyanins contain carbonyl and hydroxyl groups bound to the surface of the TiO<sub>2</sub> semiconductor layer, which helps the conduction band stimulate and transfer electrons [24].

Figure 1 shows the UV-Vis spectrum of butterfly pea extract has a specific wavelength at 573 nm with an absorbance of 0.9258, which is included in the anthocyanin wavelength range (480-580). This shows that butterfly pea extract has potential as a photosensitizer in DSSC because it has a wavelength that meets the requirements and has a high absorption value so that it can harvest photons from solar irradiation [11, 27].

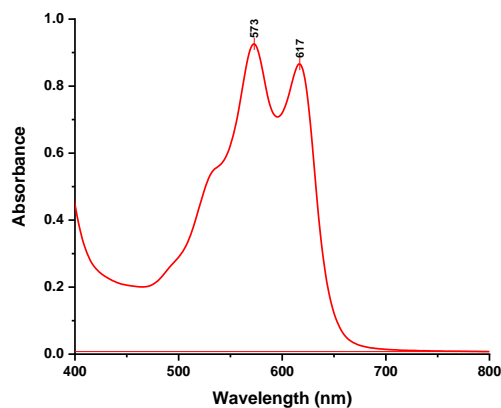
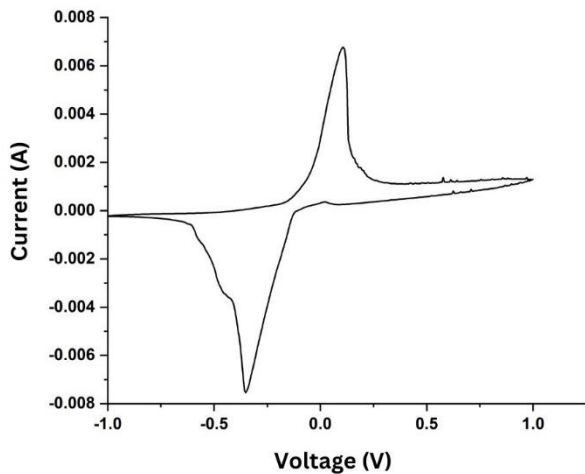


Figure 1. UV-Vis Spectrum of Butterfly Pea Photosensitizer

### Cyclic Voltammetry Analysis

Bandgap energy is the minimum energy required for electrons to excite from the valence band (HOMO) to the conduction band (LUMO) [28]. Bandgap energy is related to the electrochemical properties of the photosensitizer, which determines the potential of the dye as a photosensitizer in DSSC [29]. Band gap energy occurs in the charge separation process when the pigment absorbs photon energy from visible light. Electrons will be excited from HOMO to LUMO and then transferred to the semiconductor conduction band. The smaller the difference between the HOMO and LUMO values, the better the quality of the extracted dye. The ability to regenerate the dye indicates the ease of electron transfer from the electrolyte  $I^-/I_3^-$  to the HOMO band of the substance. This is related to the more straightforward process of excitation of dye electrons from the valence band to the conduction band. Enough energy makes the band gap energy small, and electrons can be easily excited. The conduction band is affected by TiO<sub>2</sub>, which has an effect that is in line with the LUMO of the dye, which makes it easier for electron injection [30]. The dye sensitizer-based dye in the DSSC system has a lower LUMO value requirement than the TiO<sub>2</sub> conduction band (-4.0 eV) and a lower bandgap value than the TiO<sub>2</sub> semiconductor (3.2 eV) [24].

Figure 2 is a natural dye voltammogram of butterfly pea extract, which produces the  $E_{ox}$  price from the  $I_{pa}$  value and the  $E_{red}$  price from the  $I_{pc}$  value. These prices are entered in equations 1-3, and calculations are carried out, resulting in HOMO, LUMO, and bandgap prices that meet the requirements of DSSC photosensitizers (Table 1).



**Figure 2.** Voltammogram of Butterfly Pea Photosensitizer

$$E_{LUMO} = -e (E_{ox} + 4,40)eV \tag{1}$$

$$E_{HOMO} = -e (E_{red} + 4,40)eV \tag{2}$$

$$E_g = E_{LUMO} - E_{HOMO} \tag{3}$$

**Table 1.** Results of Voltammetric Analysis of Butterfly Pea Photosensitizer

$E_{ox}$ (eV)	HOMO (eV)	$E_{red}$ (eV)	LUMO (eV)	Bandgap (eV)
0.1014	-4.5014	-0.4118	-3.9882	0.5132

**Performance of DSSC with PSf/PEG Membrane-Based Electrolyte**

Voltage and current tests were carried out by making an open circuit consisting of a resistor, multimeter, and DSSC circuit. In this measurement, the voltage and current values were observed using a multimeter on each DSSC circuit with variations in PSf/PEG composition in the membrane electrolyte. Each sample’s voltage and current measurements were plotted to determine the maximum power the DSSC can generate. Measurements were made twice, namely after assembly (0 hours) and after 72 hours. This was done to compare the efficiency and stability of DSSC with liquid electrolyte and polymer electrolyte-based PSf/PEG/DMAc membranes.

$$FF = \frac{P_{maks}}{P_T} = \frac{J_{maks}V_{maks}}{J_{sc}V_{oc}} \tag{4}$$

$$\eta = \frac{P_{out}}{P_{in}} = \frac{J_{sc}V_{oc}FF}{P_{in}} \tag{5}$$

To determine the conversion efficiency of the DSSC, calculations were made using equations 4 and 5. Using these equations shows that the efficiency value of the liquid electrolyte DSSC in the initial measurement (0 hours) is 1.66%. Membrane electrolyte-based DSSCs with variations in PSf/PEG composition from M0-M5 were 0.69, 1.11, 1.38, 1.13, 0.92, and 0.42%, respectively, at the time of initial measurement (0 hours). The DSSC efficiency value in this study is higher than the efficiency value in the research of Ludin et al. (2018), which is 0.13%, despite

using the same photosensitizer (butterfly pea extract). Figure 3 and Table 2 show that the best performance results are in DSSC with liquid electrolytes and decreased efficiency in DSSC using membrane electrolytes. The PSf/PEG membrane electrolyte-based DSSC experienced an increase in efficiency for variations M0-M2 (composition 18/0, 17/1, and 16/2), but at M3-M5 (composition 15/3, 14/4, and 13/5) it experienced a decrease in efficiency again. In this case, the liquid electrolyte DSSC has a higher efficiency than the membrane electrolyte-based DSSC due to better penetration of the liquid electrolyte into the porous TiO<sub>2</sub> layer. Several studies have also reported that the high efficiency of liquid electrolyte DSSCs is due to direct contact between the electrolyte and semiconductor without obstructing other polymers [31]. However, liquid electrolyte DSSCs can experience a significant decrease in efficiency in the long term compared to membrane electrolyte-based DSSCs. This is because the membrane functions as a liquid electrolyte trapping matrix, which results in the liquid electrolyte in the DSSC experiencing little solvent evaporation. After all, it is trapped in the membrane matrix.

Because adding PEG to the polymer composition can increase the number of pores and pore size of the membrane, due to the water-soluble nature of PEG and polymer compatibility, it can suppress the formation of microvoids [22,32]. The increase in DSSC performance (M0-M5) is due to the increase in PEG composition, which increases the number and size of membrane pores, which can increase the recombination of the PT/electrolyte interface. This resulted in the liquid electrolyte being easily trapped, thus reducing the evaporation of the liquid electrolyte solvent. The increase in membrane pore size can also increase the recombination of the PT/electrolyte interface, which impacts increasing the short circuit current ( $J_{sc}$ ). In this study, the addition of PEG reached the optimum point at M2 (PSf/PEG 16/2). The addition of PEG at M3-M5 decreased the performance of DSSC because the addition of porogen would increase the membrane pore size. A pore size that is too large will facilitate the evaporation of liquid electrolyte solvents, so electron transport has difficulty in the PT/electrolyte interface recombination mechanism, resulting in a short circuit current ( $J_{sc}$ ) that decreases with increasing PEG porogen composition [33].

The increase and decrease in DSSC performance with variations in PSf/PEG polymer composition are in line with the membrane’s main characteristics, namely selectivity and permeability values. Permeability is a membrane flow rate that is reviewed from the flux value to determine the membrane’s level of porosity (number of pores). The increase in membrane porosity affects the faster electron transport rate. On the other hand, the higher the PEG composition, the greater the particle density level, so the thrust force needed to pass particles through the membrane is significant, and the speed of the feed solution passing through the membrane is lower. Selectivity is reviewed based on the value of rejection, where the more PEG increases, the greater the membrane density, so the electron transport speed decreases [18,34].

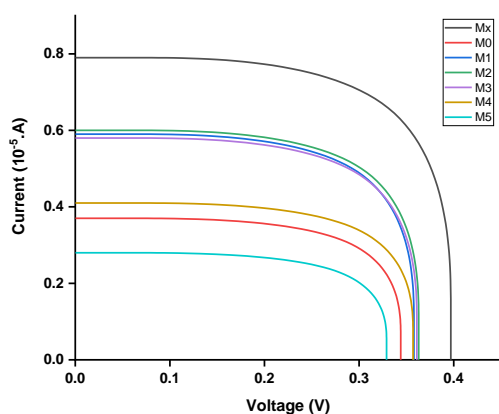


**Figure 3.** I-V Curve of DSSC in Various Electrolyte Variations for 0 Hours

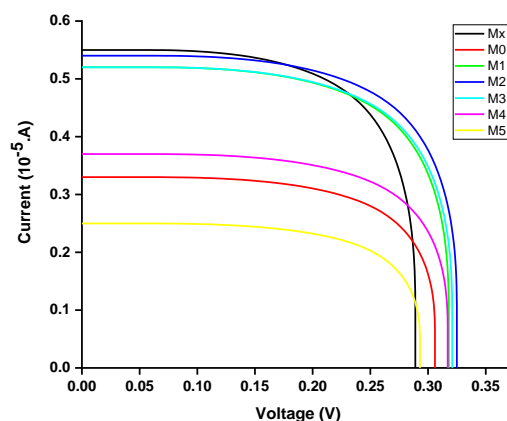


**Figure 4.** I-V Curve of DSSC in Various Electrolyte Variations for 72 Hours

**Table 2.** DSSC Photovoltaic Test Results for 0 Hours

Co-de	Composition of PSf/PEG (%)	$J_{sc}$ (A/cm <sup>2</sup> )	$V_{oc}$ (V)	FF (%)	$\eta$ (%)	Decreased $\eta$ (%)
Mx	-	$5.5 \times 10^{-5}$	0.289	71.54	0.77	53.43
M0	18/0	$3.3 \times 10^{-5}$	0.306	73.31	0.55	19.84
M1	17/1	$5.2 \times 10^{-5}$	0.318	70.95	0.89	19.75
M2	16/2	$5.4 \times 10^{-5}$	0.325	85.63	1.11	19.33
M3	15/3	$5.2 \times 10^{-5}$	0.321	72.98	0.91	19.52
M4	14/4	$3.7 \times 10^{-5}$	0.317	84.68	0.74	19.74
M5	13/5	$2.5 \times 10^{-5}$	0.293	62.31	0.34	20.17

**Table 3.** DSSC Photovoltaic Test Results for 72 Hours

Code	Composition of PSf/PEG (%)	$J_{sc}$ (A/cm <sup>2</sup> )	$V_{oc}$ (V)	FF (%)	$\eta$ (%)
Mx	-	$7.9 \times 10^{-5}$	0.397	71.54	1.66
M0	18/0	$3.7 \times 10^{-5}$	0.344	73.31	0.69
M1	17/1	$5.9 \times 10^{-5}$	0.358	70.95	1.11
M2	16/2	$6.0 \times 10^{-5}$	0.363	85.63	1.38
M3	15/3	$5.8 \times 10^{-5}$	0.361	72.98	1.13
M4	14/4	$4.1 \times 10^{-5}$	0.357	84.68	0.92
M5	13/5	$2.8 \times 10^{-5}$	0.329	62.31	0.42

The electron transfer flow rate is inversely proportional to the stability or lifetime of the DSSC. The performance stability of the liquid and polymer electrolyte DSSCs was compared by measuring the DSSCs after standing for 72 hours. Figure 4 and Table 3 show the I-V curves of DSSC and the results of DSSC performance after 72 hours. This study states that DSSC with polymer electrolyte experienced a decrease in efficiency of 19.33-20.17%, while DSSC with liquid electrolyte experienced a reduction in efficiency of 53.43%.

### Scanning Electron Microscopy (SEM) Characterization of Electrolyte Membrane

This study characterized the electrolyte membrane that produces the best performance in the DSSC system. The membrane was characterized using an SEM instrument to determine the surface morphology and cross-section. Membrane morphology affects the performance of DSSC

because, as a liquid electrolyte matrix, the membrane must have the appropriate pore size and porosity so that electron transport runs smoothly [35-36]. The results of SEM characterization on the membrane that produces the best DSSC performance (M2) can be seen in Figure 5 below.

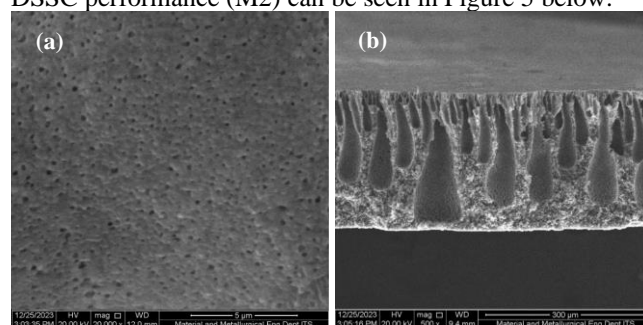


**Figure 5.** Morphology of M2 PSf/PEG/DMAc (16/2/82) Electrolyte Membrane viewed from the side of (a) Surface with 20,000x Magnification, (b) Cross Section with 500x Magnification

It was observed that the morphology of the electrolyte membrane that produced the best performance on the DSSC was the M2 membrane. The membrane has a small pore size and large porosity, as shown in the surface morphology (Figure 5a). The surface pores' nature is influenced by adding PEG to the membrane polymer. It was reported in the research of [37] that the PSf/DMAc membrane (without the addition of PEG) shows a smaller pore size and fewer pores than PSf/PEG/DMAc [37-38]. Figure 5b shows the SEM image of the cross-section of the electrolyte membrane that produces the best DSSC (M2) performance. It is shown that the M2 membrane has an asymmetric structure consisting of a dense upper surface layer (skin layer, airside) and a porous sublayer (support layer). The skin layer acts as a separation layer, and the support layer provides mechanical strength. The sublayer has visible finger-like voids under the top surface layer and large voids near the bottom of the surface layer. It was reported in the work of [38] that the size and number of finger-like pores were found to increase when the PEG composition was increased. In this study, the membrane morphology of the finger pore was found to have significant and prominent cavities. PEG is a pore shaper that forms membrane structures and can cause changes in pore size [38]. The presence of PEG in the PSf polymer solution has an effect, namely that adding PEG consumes some of the solvent and causes the polymer concentration and viscosity of the polymer solution to be higher [39]. The polymer solution is thermodynamically less stable, resulting in rapid demixing when immersed in the coagulation bath. The second effect is that PEG is hydrophilic, thus increasing the rate of entry of water diffusion in the polymer solution and forming a larger finger pore [40].

### XRD Characterization of Electrolyte Membrane

The electrolyte membrane's polymer structure was analyzed using an X-ray diffraction (XRD) instrument. Electrolyte membrane polymers have crystallinity characteristics that are important to observe because they directly affect the electrolyte's ionic conductivity in the DSSC system. An increase in the crystallinity of the electrolyte membrane polymer leads to a decrease in ionic movement through the polymer matrix [41-42]. In this study, X-ray diffraction (XRD) was performed to characterize the surface crystalline phase of the PSf/PEG/DMAc membrane that produced the best performance in DSSC (M2).

Crystallinity can affect the electron transfer properties of the membrane. The higher the crystallinity of a membrane material, the more regular the molecular arrangement of its constituent atoms. The regularity of this crystal structure facilitates electron transfer because the distance between molecules or atoms is closer and more symmetrical [43]. Electrons can more easily jump from one molecule to another in materials with a crystalline structure. High crystallinity is also related to increased membrane surface area [44]. A large surface area allows more contact between molecules, making electron transfer more efficient. However, too much crystallinity can inhibit electron transfer because its rigid and tight structure hinders electron diffusion. Therefore, the membrane requires an optimum crystallinity level to obtain maximum electron transfer [45].

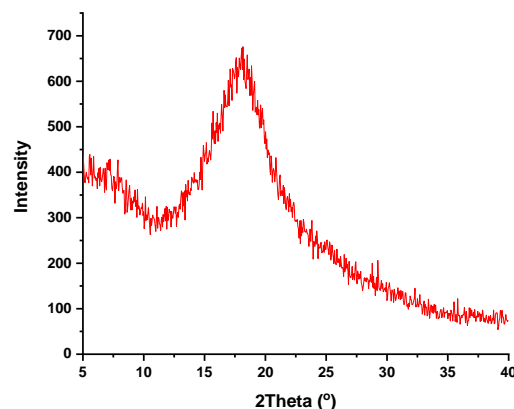


**Figure 6.** XRD Graph of Polymer Membrane M2

It can be seen in Figure 6 that the M2 membrane shows a broad peak at  $18.0626^\circ$ , which is due to hydrogen bonding as well as the formation of DMAc used as a solvent [46]. This evidence, based on the amorphous polymer's XRD results, also shows a similar peak. These peaks are due to the introduction of groups along the chain that can form hydrogen bridge bonds between and within the chains, which allows for a more ordered structure and the appearance of crystalline behavior in PSf. A suitable membrane for use as a polymer electrolyte in DSSCs has a semi-crystalline structure. A material is semi-crystalline if it has a degree of crystallinity of 35-70% [47]. In this study, the degree of crystallinity of the M2 membrane was obtained at 28.12%, which has properties close to semi-crystalline.

### Conclusion

Based on the results of the characterization of the dye sensitizer, which shows a maximum absorption wavelength of 573 nm and a bandgap of 0.5114 eV, a DSSC system was prepared with variations in the PSf/PaEG polymer electrolyte composition. Good DSSC performance is obtained from high values of open-circuit voltage ( $V_{oc}$ ), short-circuit current density ( $J_{sc}$ ), fill factor (FF), and efficiency ( $\eta$ ), but low percentage values of efficiency reduction. The research results with the best DSSC performance were DSSC with PSf/PEG membrane electrolyte composition 16/2, which produced a  $V_{oc}$  of 0.363 V,  $J_{sc}$  of  $6.0 \times 10^{-5}$  A/cm<sup>2</sup>, %FF of 85.63, and  $\eta$  of 1.33%, and a decrease in efficiency after 72 hours of 19.33%.

### Acknowledgments

The author would like to thank the Merah Putih Research Team of the Analytical Chemistry Laboratory, Department of Chemistry UNESA and all parties who have helped and supported the implementation of this research.

### References

- [1] Omar, A., Ali, M. S., & Abd Rahim, N. (2020). Electron transport properties analysis of titanium dioxide dye-sensitized solar cells (TiO<sub>2</sub>-DSSCs) based natural dyes using electrochemical impedance

- spectroscopy concept: A review. *Solar Energy (Phoenix, Ariz.)*, 207, 1088–1121.
- [2] Setyono, A. E., & Kiono, B. F. T. (2021). Dari Energi Fosil Menuju Energi Terbarukan: Potret Kondisi Minyak dan Gas Bumi Indonesia Tahun 2020 – 2050. *Jurnal Energi Baru Dan Terbarukan*, 2(3), 154–162.
  - [3] Soomar, A. M., Hakeem, A., Messaoudi, M., Musznicki, P., Iqbal, A., & Czapp, S. (2022). Solar photovoltaic energy optimization and challenges. *Frontiers in Energy Research*, 10.
  - [4] Setyawan, L. B. (2018). Perkembangan dan Prospek Sel Fotovoltaik Organik: Sebuah Telaah Ilmiah. *Techné Jurnal Ilmiah Elektroteknika*, 17(02), 93–100.
  - [5] Rosli, N., Sabani, N., Shahimin, M. M., Juhari, N., Shaari, S., Ahmad, M. F., & Zakaria, N. (2021). Dyes extracted from Hibiscus Sabdariffa flower and Pandanus amaryllifolius leaf as natural dye sensitizers by using an alcohol-based solvent. *Journal of Physics. Conference Series*, 1755(1), 012025.
  - [6] Nursam, N. M. (2020). Pengaruh material counter electrode Pada dye-sensitized solar cell. *Metalurgi*, 34(3).
  - [7] Huault, Q., Mwalukuku, V. M., Joly, D., Liotier, J., Kervella, Y., Maldivi, P., Narbey, S., Oswald, F., Riquelme, A. J., Anta, J. A., & Demadrille, R. (2020). Photochromic dye-sensitized solar cells with light-driven adjustable optical transmission and power conversion efficiency. *Nature Energy*, 5(6), 468–477.
  - [8] Li, C.-T., Kuo, Y.-L., Kumar, C. H. P., Huang, P.-T., & Lin, J. T. (2019). Tetraphenylethylene tethered phenothiazine-based double-anchored sensitizers for high performance dye-sensitized solar cells. *Journal of Materials Chemistry. A, Materials for Energy and Sustainability*, 7(40), 23225–23233.
  - [9] Liao, C., Zeng, K., Wu, H., Zeng, Q., Tang, H., Wang, L., Meier, H., Xie, Y., & Cao, D. (2021). Conjugating pillararene dye in dye-sensitized solar cells. *Cell Reports. Physical Science*, 2(2), 100326.
  - [10] Grifoni, F., Bonomo, M., Naim, W., Barbero, N., Alnasser, T., Dzeba, I., Giordano, M., Tsaturyan, A., Urbani, M., Torres, T., Barolo, C., & Sauvage, F. (2021). Toward sustainable, colorless, and transparent photovoltaics: State of the art and perspectives for the development of selective near-infrared dye-sensitized solar cells. *Advanced Energy Materials*, 11(43), 2101598.
  - [11] Kurumisawa, Y., Higashino, T., Nimura, S., Tsuji, Y., Iiyama, H., & Imahori, H. (2019). Renaissance of fused porphyrins: Substituted methylene-bridged thiophene-fused strategy for high-performance dye-sensitized solar cells. *Journal of the American Chemical Society*, 141(25), 9910–9919.
  - [12] Trivedi, M., Gupta, R., & Nirmalkar, N. (2022). Electroosmotic transport and current rectification of viscoelastic electrolyte in a conical pore nanomembrane. *Journal of Membrane Science*, 659(120755), 120755.
  - [13] Nurussaniyah, N., Anita, A., & Boisandi, B. (2018). Isolasi Dye Organik Alam dan Karakterisasinya Sebagai Sensitizer. *JIPF (Jurnal Ilmu Pendidikan Fisika)*, 3(1), 24.
  - [14] Jeyaraj, E. J., Nathan, S., Lim, Y. Y., & Choo, W. S. (2022). Antibiofilm properties of Clitoria ternatea flower anthocyanin-rich fraction towards *Pseudomonas aeruginosa*. *Access Microbiology*, 4(4).
  - [15] Widowati, W., Darsono, L., Lucianus, J., Setiabudi, E., Susang Obeng, S., Stefani, S., Wahyudianingsih, R., Reynaldo Tandibua, K., Gunawan, R., Riski Wijayanti, C., Novianto, A., Sari Widya Kusuma, H., & Rizal, R. (2023). Butterfly pea flower (*Clitoria ternatea* L.) extract displayed antidiabetic effect through antioxidant, anti-inflammatory, lower hepatic GSK-3 $\beta$ , and pancreatic glycogen on Diabetes Mellitus and dyslipidemia rat. *Journal of King Saud University. Science*, 35(4), 102579.
  - [16] Ludin, N. A., Al-Alwani, M. A. M., Mohamad, A. B., Kadhum, A. A. H., Hamid, N. H., Ibrahim, M. A., Teridi, M. A. M., Ali Al-Hakeem, T. M., Mukhlus, A., & Sopian, K. (2018). Utilization of natural dyes from Zingiber officinale leaves and Clitoria ternatea flowers to prepare new photosensitizers for dye-sensitized solar cells. *International Journal of Electrochemical Science*, 13(8), 7451–7465.
  - [17] Pramananda, V., Hadyan Fityay, T. A., & Misran, E. (2021). Anthocyanin as natural dye in DSSC fabrication: A review. *IOP Conference Series: Materials Science and Engineering*, 1122(1), 012104.
  - [18] Kusumawati, Nita, Setiarso, P., Santoso, A. B., Muslim, S., A'yun, Q., & Putri, M. M. (2023). Characterization of poly(vinylidene fluoride) nanofiber-based electrolyte and its application to dye-sensitized solar cell with natural dyes. *Indonesian Journal of Chemistry*, 23(1), 113.
  - [19] Bekele, E. T., & Sintayehu, Y. D. (2022). Recent progress, advancements, and efficiency improvement techniques of natural plant pigment-based photosensitizers for dye-sensitized solar cells. *Journal of Nanomaterials*, 2022, 1–35.
  - [20] Serbanescu, O. S., Voicu, S. I., & Thakur, V. K. (2020). Polysulfone functionalized membranes: Properties and challenges. *Materials Today. Chemistry*, 17(100302), 100302.
  - [21] Kusumawati, N., Setiarso, P., & Muslim, S. (2018). Polysulfone/polyvinylidene fluoride composite membrane: Effect of coating dope composition on membrane characteristics and performance. *Rasayan Journal of Chemistry*, 11(3), 1034–1041.
  - [22] Lin, Y.-C., Tseng, H.-H., & Wang, D. K. (2021). Uncovering the effects of PEG porogen molecular weight and concentration on ultrafiltration membrane properties and protein purification performance. *Journal of Membrane Science*, 618(118729), 118729.
  - [23] Silva, C., Santos, A., Salazar, R., Lamilla, C., Pavez, B., Meza, P., Hunter, R., & Barrientos, L. (2019). Evaluation of dye sensitized solar cells based on a pigment obtained from Antarctic *Streptomyces fildesensis*. *Solar Energy (Phoenix, Ariz.)*, 181, 379–385.
  - [24] Hayat, A., Putra, A. E. E., Amaliyah, N., & Pandey, S. S. (2019). Clitoria ternatea flower as natural dyes for Dye-sensitized solar cells. *IOP Conference Series. Materials Science and Engineering*, 619(1), 012049.

- [25] Tang, R., He, Y., & Fan, K. (2023). Recent advances in stability improvement of anthocyanins by efficient methods and its application in food intelligent packaging: A review. *Food Bioscience*, 56(103164), 103164.
- [26] Syafa'atullah, A. Q., Amira, A., Hidayati, S., & Mahfud, M. (2020). Anthocyanin from butterfly pea flowers (*Clitoria ternatea*) by ultrasonic-assisted extraction. *THE 14TH JOINT CONFERENCE ON CHEMISTRY 2019*.
- [27] Grifoni, F., Bonomo, M., Naim, W., Barbero, N., Alnasser, T., Dzeba, I., Giordano, M., Tsaturyan, A., Urbani, M., Torres, T., Barolo, C., & Sauvage, F. (2021). Toward sustainable, colorless, and transparent photovoltaics: State of the art and perspectives for the development of selective near-infrared dye-sensitized solar cells. *Advanced Energy Materials*, 11(43), 2101598.
- [28] Adawiyah, D. R., Departemen Ilmu dan Teknologi Pangan, Fakultas Teknologi Pertanian, Institut Pertanian Bogor, Bogor, Indonesia, Muhandri, T., Subarna, S., Sugiyono, S., & Departemen Ilmu dan Teknologi Pangan, Fakultas Teknologi Pertanian, Institut Pertanian Bogor, Bogor, Indonesia. (2019). Pengaruh Fortifikasi Zat Besi Menggunakan Fe-Sulfat, Fe-Fumarat dan Na Fe EDTA Terhadap Kualitas Sensori Produk-Produk Olahan Tepung Terigu. *Jurnal Mutu Pangan: Indonesian Journal of Food Quality*, 6(2), 54–62.
- [29] Vasanthi, D. S., Ravichandran, K., Kavitha, P., Sriram, S., & Praseetha, P. K. (2020). Combined effect of Cu and N on bandgap modification of ZnO film towards effective visible light responsive photocatalytic dye degradation. *Superlattices and Microstructures*, 145(106637), 106637.
- [30] Çakar, S., Atacan, K., & Güy, N. (2019). Synthesis and characterizations of TiO<sub>2</sub>/Ag photoanodes for used indigo carmine sensitizer based solar cells. *Celal Bayar Üniversitesi Fen Bilimleri Dergisi*, 23–29.
- [31] Chalkias, D. A., Verykokkos, N. E., Kollia, E., Petala, A., Kostopoulos, V., & Papanicolaou, G. C. (2021). High-efficiency quasi-solid state dye-sensitized solar cells using a polymer blend electrolyte with "polymer-in-salt" conduction characteristics. *Solar Energy (Phoenix, Ariz.)*, 222, 35–47.
- [32] Nur-E-Alam, M., Deowan, S. A., Hossain, E., Hossain, K. S., Miah, M. Y., & Nurnabi, M. (2024). Fabrication of polysulfone-based microfiltration membranes and their performance analysis. *Water, Air, and Soil Pollution*, 235(1).
- [33] Selvanathan, V., Yahya, R., Alharbi, H. F., Alharthi, N. H., Alharthi, Y. S., Ruslan, M. H., Amin, N., & Akhtaruzzaman, M. (2020). Organosoluble starch derivative as quasi-solid electrolytes in DSSC: Unravelling the synergy between electrolyte rheology and photovoltaic properties. *Solar Energy (Phoenix, Ariz.)*, 197, 144–153.
- [34] Liu, Q., Gao, N., Liu, D., Liu, J., & Li, Y. (2018). Structure and photoelectrical properties of natural photoactive dyes for solar cells. *Applied Sciences (Basel, Switzerland)*, 8(9), 1697.
- [35] Lai, T., & Qu, Z. (2023). Pore-scale parametric sensitivity analysis of liquid water transport in the gas diffusion layer of polymer electrolyte membrane fuel cell. *Applied Thermal Engineering*, 229, 120616.
- [36] Trivedi, M., Gupta, R., & Nirmalkar, N. (2022). Electroosmotic transport and current rectification of viscoelastic electrolyte in a conical pore nanomembrane. *Journal of Membrane Science*, 659(120755), 120755.
- [37] Alasfar, R. H., Kochkodan, V., Ahzi, S., Barth, N., & Koç, M. (2022). Preparation and characterization of polysulfone membranes reinforced with cellulose nanofibers. *Polymers*, 14(16), 3317.
- [38] He, M., Li, T., Hu, M., Chen, C., Liu, B., Crittenden, J., Chu, L.-Y., & Ng, H. Y. (2020). Performance improvement for thin-film composite nanofiltration membranes prepared on PSf/PSf-g-PEG blended substrates. *Separation and Purification Technology*, 230(115855), 115855.
- [39] Ahmad, T., Guria, C., & Mandal, A. (2020). Kinetic modeling and simulation of non-solvent induced phase separation: Immersion precipitation of PVC-based casting solution in a finite salt coagulation bath. *Polymer*, 199, 122527.
- [40] Folgado, E., Ladmiral, V., & Semsarilar, M. (2020). Towards permanent hydrophilic PVDF membranes. Amphiphilic PVDF-b-PEG-b-PVDF triblock copolymer as membrane additive. *European Polymer Journal*, 131, 109708.
- [41] Amalia, R., & Elvian Gayuh Prasetya, H. (2023). Membran Elektrolit Polimer Kitosan-Polyvinil Alkohol pada Direct Methanol Fuel Cell. *Journal of Research and Technology*, 8(2).
- [42] Chitsazan, A., & Monajje, M. (2020). Increasing the efficiency Proton exchange membrane (PEMFC) & other fuel cells through multi graphene layers including polymer membrane electrolyte. *French-Ukrainian Journal of Chemistry*, 8(1), 95–107.
- [43] Jeedi, V. R., Narsaiah, E. L., Yalla, M., Swarnalatha, R., Reddy, S. N., & Sadananda Chary, A. (2020). Structural and electrical studies of PMMA and PVdF based blend polymer electrolyte. *SN Applied Sciences*, 2(12).
- [44] Wang, J., Wang, L., Tiang, M., Tao, Y., Zou, Y., Yang, Y., Wen, Z., Liu, X., Wang, M., Li, L., Wang, D., & Gao, D. (2023). Fabrication of High-Crystallinity Covalent Organic Framework and Its Nylon Based Membrane: Application in the Enrichment and Interception of Dyes. *Journal of Environmental Chemical Engineering*, 11, 110989.
- [45] Zhang, Y., Miller, M. T., Boldt, R., & Stommel, M. (2023). *Crystallinity Effect on Electron-Induced Molecular Structure Transformations In Additive-Free PLA*.
- [46] Zahir, M. H., Rahman, M. M., Irshad, K., & Rahman, M. M. (2019). Shape-stabilized phase change materials for solar energy storage: MgO and Mg(OH)<sub>2</sub> mixed with polyethylene glycol. *Nanomaterials (Basel, Switzerland)*, 9(12), 1773.
- [47] Kalel, S., & Wang, W. C. (2023). Optical properties of PVDF-TrFE and PVDF-TrFE-CTFE films in terahertz band. *Materials Research Express*, 10(4).